https://doi.org/10.18524/1810-4215.2023.36.290586

MOTIONS OF THE COMPONENTS OF AGNS ACCORDING TO VLBI MOJAVE DATA AS INDICATORS OF THE ACTIVITY AND SPATIAL STRUCTURE OF THE JET

Zabora D.[1], Ryabov M.[2], Sukharev A.[2], Bezrukovs V.[3], Bazyey A.[1]

[1] Faculty of Mathematics, Physics and Information Technologies ONU, Ukraine

[2] Institute of Radio Astronomy of the National Academy of Sciences of Ukraine (IRA NASU), Ukraine

[3] Ventspils International Radioastronomy Centre of Ventspils University of Applied Sciences, Latvia

ABSTRACT. The system of ten radio telescopes VLBA (Very Large Baseline Array), with a maximum baseline of about 8,600 km, of the National Radio Astronomy Observatory of the USA (NRAO USA) carries out systematic monitoring observations of about 500 active galactic nuclei (AGN), the results are presented in the MOJAVE database. The resulting angular resolution (~0.47 arcseconds at a frequency of 15.4 GHz) is enough to separate the close surroundings of the AGN and its jet. The results of corresponding observations make it possible to compare the features of movement in the jet with the processes of activity of the AGN, as well as to study its spatial structure.

The MOJAVE database contains the spectral densities of the radio fluxes of the AGN, radio images for each epoch of observations at the frequency of 15.4 GHz, and "Separation jet" diagrams (showing the angular separation of the jet components over time). This information makes it possible to study the movement of these components. In this work, a general analysis of movement patterns of the components of the 3C 273 jet was performed. In the published papers of the MOJAVE team, a similar analysis wasn't presented for all jet's features.

Keywords: Active galactic nucleus**,** Separation jet, Relativistic jet, 3C 273, variations.

АННОТАЦІЯ. Система з десяти радіотелескопів VLBA (Very Large Baseline Array), з максимальною довжиною бази близько 8,600 км, Національної Радіоастрономічної Обсерваторії США (NRAO USA) проводить систематичні моніторингові спостереження близько 500-та активних ядер галактик (АЯГ), результати яких представлені у базі даних MOJAVE. Результуючої кутової роздільної здатності (~0.47 тисячних кутової секунди на частоті у 15.4 ГГц) достатньо для розділення близького оточення АЯГ та його джета. Результати відповідних спостережень дозволяють зіставляти особливості руху у джеті з процесами активності АЯГ, а також вивчати його просторову структуру.

У базі даних MOJAVE представлені спектральні щільності радіопотоків АЯГ, радіозображення на кожну епоху спостережень на частоті 15.4 ГГц та діаграми "Separation jet" (що демонструють кутове відхилення компонент джета у часі). Ця інформація й дозволяє вивчати рух цих компонент. У цій роботі, було проведено загальний аналіз патернів руху компонент джета 3C 273. В опублікованих статтях команди MOJAVE, подібний проведеному аналіз не було представлено для усіх особливостей джетів.

Ключові слова: Активні ядра галактик, розділений джет, релятивістський джет, 3C 273, змінність.

1. Introduction

The high level of radiation and kinetic energy of the Active Galactic Nuclei (AGN) jets is provided by active processes in the "accretion disk – core – jet" system. According to the AGN standard model (Fig. 1), the source of its huge energy release is the gravitational energy of an accretion disk matter, which falls on the supermassive black hole in the center. The accretion disk is formed from surrounding matter (gas clouds, stars) that falls on the central supermassive black hole. The core is the region where matter is injected into the jet. Here active processes, that lead to the appearance of jets, are realized.

A common phenomenon for AGNs are relativistic jets — collimated jets of relativistic plasma that are ejected in a direction (mostly) perpendicular to the plane of accretion disk and are observed at distances up to tens or hundreds of kiloparsecs from the core.

Behind the disk plane there is a dust torus, which makes a significant contribution to the IR emission of many AGNs.

The use of aperture synthesis systems and VLBI observations in radio astronomy (including space radio telescopes) has made it possible to study the structure of jets and the processes occurring there. They include the presence of compact plasma releases from the core, shock waves, plasma flows, standing knots, etc. Currently, the

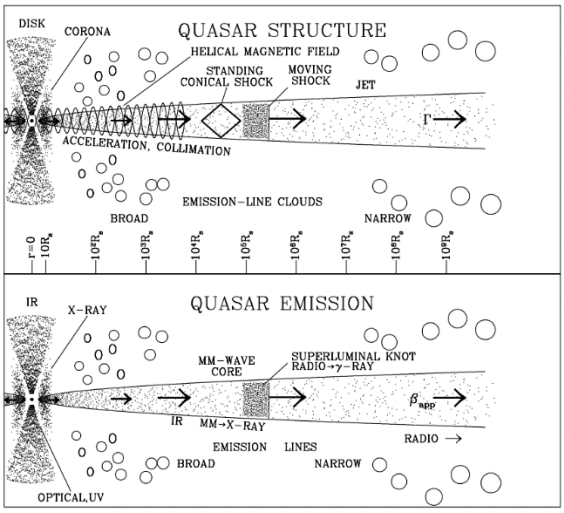

Figure 1: Scheme of an AGN structure (Marcher, 2009)

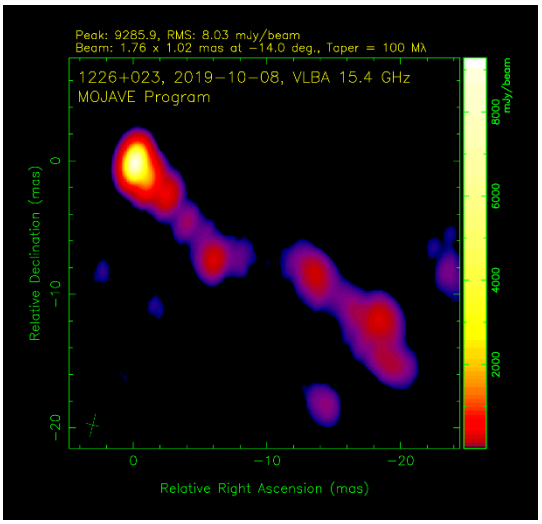

Figure 2: Parsec-scale radio image of 3C 273 obtained from the MOJAVE VLBI observing program database

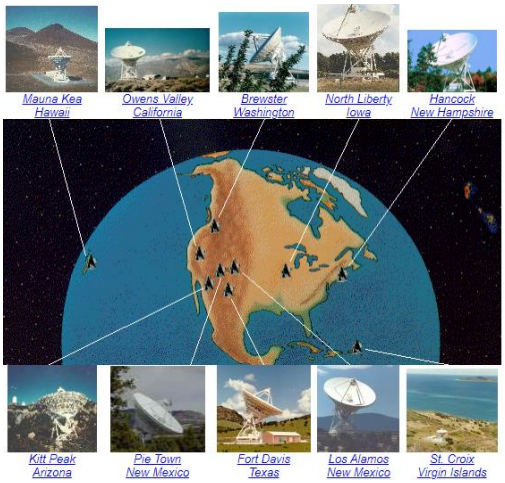

Figure 3: Very Long Baseline Antenna Array (VLBA)

structure of jets is also being studied using orbital space telescopes in the optical, X-ray, infrared and gamma-ray bands (Hubble and Webb Space Telescopes, Chandra X-ray Space Telescope, etc.).

The mechanism by which the matter of the accretion disk is accelerated to relativistic speeds, leading to the formation of jets, remains a subject of debate (especially if we are talking about a specific source), but the most likely mechanisms are those associated with strong magnetic fields in the vicinity of the black hole and its rotation. Particularly notable are the Blandford-Znajek (Blandford & Znajek, 1997) and Blandford-Payne (Blandford & Payne) processes.

The BZ process can serve as a mechanism for the rotational energy of a black hole extraction through its magnetosphere, while the BP process can serve as a mechanism for extracting the rotational energy of an accretion disk through the MHD process. However, the processes of jet formation under various conditions of interaction between the accretion disk and the black hole are studied in more detail using numerical calculations within MHD approach, generalized to the case of general relativity (for additional information, please refer to Yosuke, 2022).

Shock waves that appear as a result of ejections of matter into the jet and manifestation of core activity, as well as magnetic fields in the jet, accelerate relativistic particles that produce synchrotron radiation (mainly in the radio band) (Marcher, 2009). Overall, all these processes form the observed radio image of the core-jet system (Fig. 2).

Active galactic nuclei and their jets aren't isolated systems. The surrounding galactic and extragalactic medium have a direct influence on AGN and jets. As the results of numerical simulations show, galactic matter feeds the central engine, and extragalactic medium (and galactic too) can slow down the particles of the jet's matter, as a result significantly shortening it or even preventing its formation (Tanner & Weaver, 2022).

Active galactic nuclei include objects such as radio galaxies, Seyfert galaxies, quasars and blazars. The difference between them, in general terms, is explained by the orientational unification AGN model due to the different angles of disk-jet system to the observer's line of sight. The blazar is observed when the angle of the radio loud jet is close to the line of sight. Otherwise, if there is the loud radio jet, a quasar (one-sided jet) or a radio galaxy (when relativistic jets are visible from both poles of the disk) is observed. If there is a weak jet, Seyfert (I or II type) is observed (Urry & Padovani, 1995).

2. VLBI program for monitoring active galactic nuclei jets (MOJAVE)

The monitoring of relativistic jets of AGNs (MOJAVE) program has a database of ~500 radio sources (radio galaxies, quasars, blazars, Seyfert galaxies) observed by the VLBA radio interferometer of the National Radio Astronomy Observatory (NRAO USA).

VLBA is a radio interferometric network of ten 25-meter radio telescopes of the same design. Observations are carried out at frequencies from 0.3 GHz – 96 GHz with the largest base of 8.611 km, which allows achieving angular resolutions up to 0.17 – 22 thousandths of an arc second (https://public.nrao.edu/telescopes/vlba/).

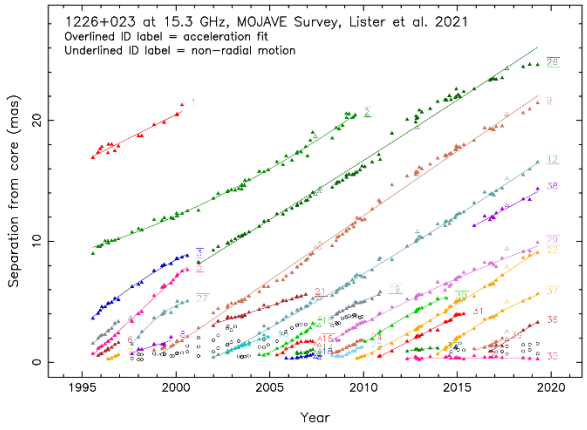

Figure 4: Diagram of Separation jet of the 3C 273

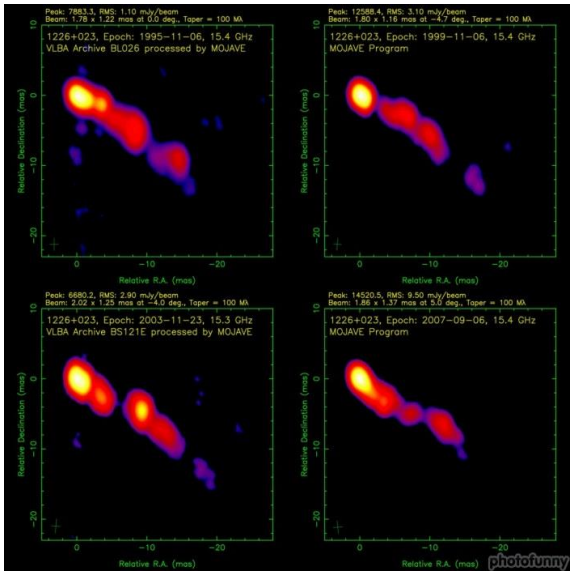

Figure 5: Evolution of 3C 273 radio images over time

Based on the interferometric picture that is taken as a result of observations by the VLBA network, the image is restored by fitting Gaussian surfaces into the brightest ejected components. The accuracy of image reconstruction is confirmed by cross-identification between epochs and authors. The entire process of obtaining radio images is described in detail in the papers (Lister et al., 2009; 2019; 2021).

The MOJAVE database contains both radio images of active nuclei with their jets at a frequency of 15.4 GHz and "Separation jet" diagrams (for most radio sources, Fig. 4). They represent the angular separation of individual components (marked in different colors) from the core over time (https://www.cv.nrao.edu/MOJAVE/allsources.html).

3. Research results of quasar 3C 273

The subject of research in this paper is the kinematics of jet based on the "Separation jet" diagram of the quasar 3C 273 from the MOJAVE VLBI monitoring database. The observational data obtained by the MOJAVE team allow a detailed analysis of the variability of the spatial structure of its jet. In Fig. 5, VLBI radio images of 3C 273 are shown with an interval of ~4 years between "neighbouring" ones. They show the ejection of bright components into the jet, their movement and escape from visibility over time.

The "Separation jet" diagram of quasar 3C 273 in Figure 4 is very representative, since it contains both moving components and slow and stationary ones.

Quasar 3C 273 is located in the constellation Virgo at $z \sim 0.1576$ redshift and is one of the most actively studied AGNs, as well as one of the closest and brightest quasars (Schmidt, 1963).

A team of authors (Ryabov et al., 2016) carried out studies of this object to identify the main periods of radio flux variability based on monitoring observations from the Michigan Radio Astronomy Observatory using wavelet analysis approach. Subsequently, in paper (Zabora et al., 2022), using observational data on variations of the core flux of this source according to MOJAVE data, changes in the core and jet fluxes were separated. The article (Volvach et al., 2023) considers the possibility of the presence of a binary black hole in 3C 273, and also calculated the masses of black holes in the binary system based on quasiperiods of variability of radio fluxes at different frequencies. The results of these calculations are in good agreement with calculations based on spectroscopic observations (Paltani & Turler, 2005).

Many works have been dedicated to the study of the kinematics and structure of the 3C 273 jet. For example, in work (Okino et al., 2022) the kinematics of the jet and the break of its collimation were researched, a similar was studied in work (Akiyama et al., 2018). In paper (Savolainen et al., 2006), was considered the velocity gradient in the direction perpendicular to the jet axis, and the non-ballistic motion of certain components was also determined. The article (Qian et al., 2001) discusses variations of the Lorentz factor of jet 3C 273 and also proposes descriptive models.

Also, the kinematics of the components of AGN jets of a large sample was descripted by participants in the MOJAVE program in a series of articles (Lister et al., 2009; 2019; 2021). In these works, a general statistical analysis was carried out, the methodology for constructing radio images, "Separation jet" diagrams, etc. was described.

4. Results of research of the "core-jet" system kinematics of 3C 273

For the 3C 273 quasar, from the "Separation jet" diagram, an angular distance of components (from the core) of its jet in time were obtained. A total of 31 components were studied over a 25-year observation period from 1995 to 2020 (Fig. 4). For each of them the speed of their radial motion in the jet was determined. The results are presented in Table 1.

The table shows the observation time interval for each of the components, their average speed $\bar{V}$ in thousandths

of arcsec per year; average speed for the jet in the same units $\langle\bar{V}\rangle$; relative deviation of the average for the component from the average for the jet $\frac{\bar{V}-\langle\bar{V}\rangle}{\langle\bar{V}\rangle}$; amplitude velocities for a component $V_{\max}, V_{\min}$ and their corresponding relative deviations from the average for the same component $\frac{V_{\max,\min}-\bar{V}}{\bar{V}}$.

Table 1: Main parameters of the components of jet 3C 273.

№	Observation interval, years	$\bar{V}$, $\frac{mas}{year}$	$\frac{\bar{V}-\langle\bar{V}\rangle}{\langle\bar{V}\rangle}$	$V_{\max}$, $\frac{mas}{year}$	$\frac{V_{\max}-\bar{V}}{\bar{V}}$	$V_{\min}$, $\frac{mas}{year}$	$\frac{V_{\min}-\bar{V}}{\bar{V}}$
1	1995.57 – 2000.32	0.79	-0.02	3.60	3.54	-3.22	-5.05
2	1995.57 – 2009.56	0.78	-0.03	8.57	9.94	-7.96	-11.15
3	1995.57 – 2000.61	1.04	0.28	3.15	2.03	-0.48	-1.47
4	1995.57 – 1996.93	1.31	0.62	2.63	1.01	0.23	-0.83
5	1995.57 – 2000.61	1.44	0.78	2.23	0.55	0.33	-0.77
6	1995.84 – 1996.93	1.00	0.24	1.48	0.48	0.45	-0.55
7	1996.37 – 1996.93	0.66	-0.19	1.02	0.55	0.30	-0.55
8	1997.65 – 1999.73	0.54	-0.34	1.51	1.80	-0.14	-1.27
9	1998.83 – 2019.28	1.06	0.31	5.42	4.09	-2.65	-3.49
12	2001.99 – 2019.28	0.93	0.15	6.46	5.92	-2.91	-4.11
13	2002.74 – 2004.92	0.60	-0.26	1.45	1.41	-0.68	-2.12
15	2004.44 – 2007.29	0.90	0.11	3.02	2.35	-0.20	-1.22
16	2005.37 – 2007.29	0.62	-0.23	2.05	2.30	-0.27	-1.44
17	2006.45 – 2007.29	0.30	-0.63	0.79	1.67	-0.22	-1.76
18	2005.87 – 2007.29	0.23	-0.71	0.88	2.74	-0.03	-1.14
19	2008.33 – 2010.89	0.73	-0.10	4.00	4.50	-0.80	-2.10
21	2001.99 – 2006.92	0.50	-0.38	1.43	1.87	-0.65	-2.31
22	2009.62 – 2019.28	0.92	0.14	2.18	1.37	0.26	-0.71
24	2008.33 – 2009.93	0.71	-0.12	2.60	2.64	0.27	-0.62
25	2008.33 – 2009.92	0.51	-0.37	2.80	4.47	-0.63	-2.23
26	2001.2 – 2019.29	0.99	0.22	12.57	11.73	-6.27	-7.35
27	1997.65 – 2000.61	1.18	0.45	2.64	1.24	0.18	-0.85
29	2008.33 – 2019.29	0.72	-0.11	7.61	9.50	-2.28	-4.14
30	2010.07 – 2014.42	0.88	0.09	2.44	1.77	0.06	-0.93
31	2010.82 – 2015.35	0.81	0.00	1.73	1.13	-0.26	-1.32
32	2012.33 – 2013.95	0.16	-	0.60	-	-0.63	-
35	2012.32 – 2019.28	0.00	-	0.86	-	-2.52	-
36	2016.74 – 2019.28	0.98	0.21	2.20	1.26	-0.20	-1.21
37	2013.96 – 2019.28	0.93	0.15	2.82	2.03	0.27	-0.71
38	2015.9 – 2019.28	0.83	0.03	2.80	2.38	-1.11	-2.34
39	2015.9 – 2017.39	0.58	-0.28	1.38	1.36	0.21	-0.64
$\langle\bar{V}\rangle = 0.81$			$\frac{s_{\bar{V}}}{\langle\bar{V}\rangle} = 0.34$	$\left\langle\left\lvert\frac{V_{\max}-\bar{V}}{\bar{V}}\right\rvert\right\rangle = 3.02$		$\left\langle\left\lvert\frac{V_{\min}-\bar{V}}{\bar{V}}\right\rvert\right\rangle = 2.22$	

At the end of table, the standard deviation $s_{\bar{V}}$ of the average velocity of components from the average for jet, normalized to the average speed over the jet $\langle \bar{V} \rangle$, is placed. It is indicative in the context of dispersion of the velocities of the components in the jet.

The average absolute deviations of amplitude velocities $\left\langle \left| \frac{V_{\max,\min} - \bar{V}}{\bar{V}} \right| \right\rangle$ of the components are also placed. Despite the somewhat complex concept, they are indicative in the context of spread of velocities for one component on average over the jet.

Stationary and slow-moving components ($\bar{V} <\sim 0.2$ *mas / year*) were not taken into account when calculating the values at the end of the table.

The results show a predominance of moving components. Stationary and slow-moving components in the picture plane are presented: No. 32 and 35 according to MOJAVE numbering.

The standard deviation of the average velocities shows significant variation in velocities between components. However, the speed of the component varies, as a rule, by an order of magnitude greater than the average speed of the components in the jet.

Figure 6 shows a histogram of the distribution of average velocities of the moving components (except for the 32nd and 35th) in comparison with the normal distribution with parameters $\langle \bar{V} \rangle = 0.81$ and $s_{\bar{V}} = 0.28$. The observed distribution is close to normal. This may indicate that the process of ejection of components into the jet is quasi-regular.

Fig. 7, 8 show diagrams of distributions of peak (maximum/minimum) velocities of the components of jet 3C 273. They are showing significant asymmetry ($A_S^{V_{\max}} \sim 2.1$, $A_S^{V_{\min}} \sim -2.3$).

The overwhelming majority of events associated with the achievement of maximum speed by the jet components are in the range of up to 4 $mas/year$.

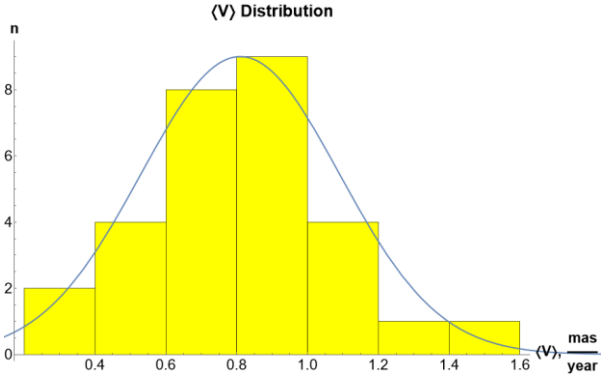

Figure 6: Distribution of average velocities of the moving components of jet 3C 273

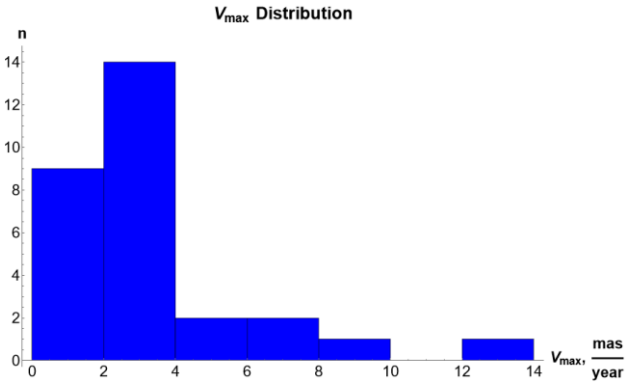

Figure 7: Distribution of maximum velocities of the moving components of jet 3C 273

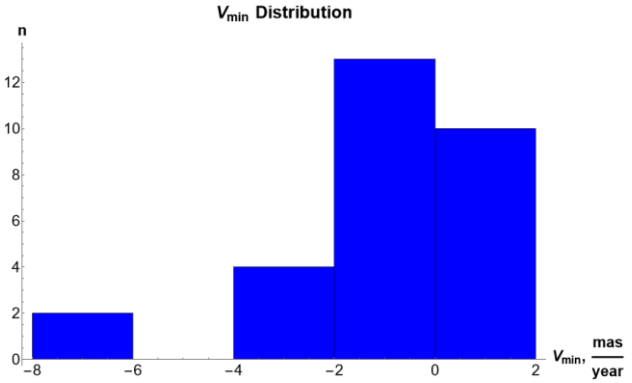

Figure 8: Distribution of minimum velocities of the moving components of jet 3C 273

Higher velocities occur sporadically and will be the subject of further research.

The values of the minimum component velocities may reflect braking processes in jets. The overwhelming number of such events correspond to speed intervals (-2 to +2), which may reflect the presence of a quasi-regular structure of the jet, which determines the deceleration of the movement of the components.

5. Features of the motion kinematics of individual components of jet 3C 273

Farther, to determine the average values of the angular velocity of movement of some components, a single three points linear smoothing was performed. This allows to reduce the influence of random errors on its values.

The 2nd component (Fig. 9) over 15 years shows a monotonic increase in angular velocity on average 0.79 $\frac{mas}{year}$ with an acceleration of 0.02 $\frac{mas}{year^2}$.

A smoothed diagram of the dependence of angular velocity on time shows the variable nature of its changes: we can suspect its three-year cyclicity. From 1996 to 1999, the angular velocity was 0.68 $\frac{mas}{year}$, from 2000 to

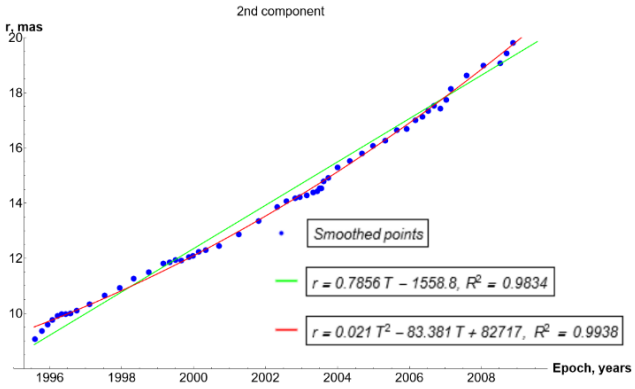

Figure 9: Smoothed "Separation jet" for the 2nd component, comparison with linear and quadratic approximation of the initial points

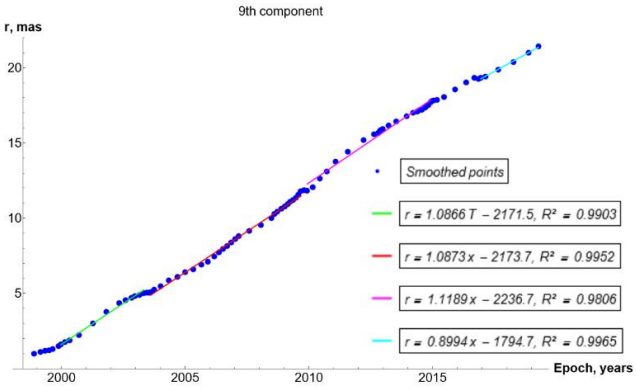

Figure 11: Smoothed "Separation jet" for the 9th component, comparison with piecewise linear approximation

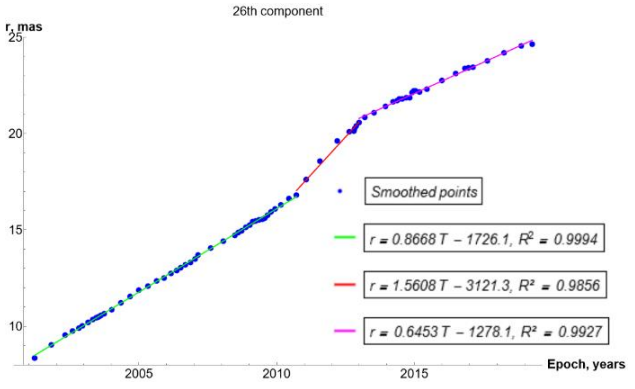

Figure 10: Smoothed "Separation jet" for the 26th component, comparison with piecewise linear approximation

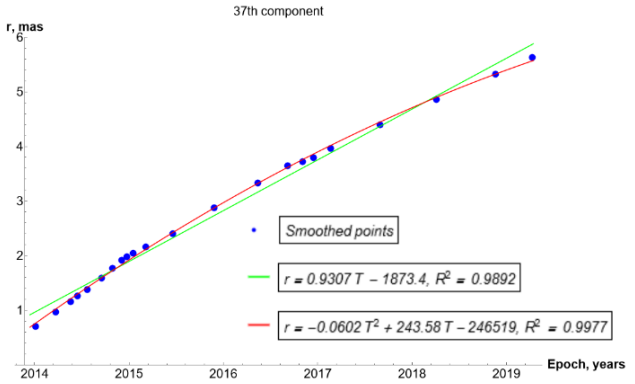

Figure 12: Smoothed "Separation jet" for the 37th component, comparison with linear and quadratic approximation of the original points

2003, the angular velocity was 0.73 $\frac{mas}{year}$, from 2003 to 2006, 0.90 $\frac{mas}{year}$, from 2006 to 2009, 1.09 $\frac{mas}{year}$. In 1996, 1999, 2003, 2006 and 2009 there are time intervals of the order of a month, during which the angular velocity of the component is nearly unchanged.

The 26th (Fig. 10) component in 2001-2010 moves with a constant angular velocity of 0.87 $\frac{mas}{year}$, then the speed increases to 1.56 $\frac{mas}{year}$, but in 2013 it decreases to 0.65 $\frac{mas}{year}$.

The 9th (Fig. 11) component during the observation period shows a changing angular velocity: in 2001-2003 it was 1.09 $\frac{mas}{year}$, then a significant slowdown follows. Speed returns to 1.09 $\frac{mas}{year}$ in 2003-2009, in 2009 the component almost stops. From 2009 to the end of 2012, the angular velocity is about 1.12 $\frac{mas}{year}$. From the end of 2012 to 2019, the angular velocity decreases on average to 0.90 $\frac{mas}{year}$.

The 37th (Fig. 12) component moves with an average speed of 0.93 $\frac{mas}{year}$, but throughout the entire observation interval the angular velocity decreases with an acceleration of 0.06 $\frac{mas}{year^2}$.

6. Conclusion

The MOJAVE project has unique data from long-term monitoring observations of a sample of ~500 active galactic nuclei, which make it possible to study the variability and structures of them and their jets. In this work, the kinematics of the jet components of the quasar 3C 273 was studied. A number of results were obtained:

1. Data were obtained on the angular distances from the core of the 31 components of jet 3C 273 on the observation epochs for the 1995 – 2020-time interval (~25 years) for further calculation of their velocities and the dynamics of their changes.
2. The "Separation jet" diagram demonstrates the presence of both stationary/slow and fast components, the number of which predominates. Calculations show that the average velocities of the jet components differ significantly from each

other. However, not as much as the velocities of the components themselves change.

3. The average component velocities have a distribution that is close to normal, this can reflect quasiregular nature of core activity.
4. The nature of minimum/maximum component velocities changes don't correspond to the normal distribution and correspond to episodic processes of manifestation of AGN activity and variations in the spatial structure of the jet.
5. The individual features of changes in velocities of the selected components of jet 3C 273 were analyzed. They demonstrate episodes of acceleration, braking and stationary states. Thus, the components of the jet are also "test bodies" that reflect the spatial structure of the magnetic fields in the jet.

References

Akiyama K., Asada K., Fish V. et al.: 2018, *Galaxies*, **6**, 15. https://doi.org/10.3390/galaxies6010015

Blandford R. D., Znajek R. L.: 1977, *MNRAS*, **179**, 433. https://doi.org/10.1093/mnras/179.3.433

Blandford, R.D., Payne, D.G.: 1982, *MNRAS*, **199**, 883. https://doi.org/10.1093/mnras/199.4.883

Hiroki O., Kazunori A., Keiichi A. et al.: 2022, *ApJ*, **940**, 17. https://doi.org/10.3847/1538-4357/ac97e5

Lister M.L., Cohen M.H., Homan D.C. et al.: 2009, *AJ*, **138**, 1874. https://doi.org/10.1088/0004-6256/138/6/1874

Lister, M. L., Homan, D. C., Hovatta, T. et al.: 2019, *ApJ*, **874**, 19. https://doi.org/10.3847/1538-4357/ab08ee

Lister M.L., Homan D.C., Kellermann K.I. et al: 2021, *ApJ*, **923**, 19. https://doi.org/10.3847/1538-4357/ac230f

Marcher A.P.: 2009, eprint (arXiv:0909.2576) https://doi.org/10.48550/arXiv.0909.2576

Paltani, S., Türler, M.: 2005, *A&A*, **435**, 811. https://doi.org/10.1051/0004-6361:20041206

Qian, S., Zhang Xi., Krichbaum T.P. et al.: 2001, *Chin. J. Astron. Astrophys.*, **1**, 236. doi:10.1088/1009-9271/1/3/236

Ryabov M.I., Sukharev A.L., Donskikh A.I.: 2016, *Radio physics and radio astronomy*, **21**, 161.

Savolainen, T., Wiik, K., Valtaoja, E. et al: 2006, *A&A*, **446**, 71. https://doi.org/10.1051/0004-6361%3A20053753

Schmidt, M.: 1963, *Nature*, **197**, 1040. https://doi.org/10.1038/1971040a0

Tanner R., Weaver K.A.: *AJ*, **163**, 17. https://doi.org/10.3847/1538-3881/ac4d23

Urry, C. M., Padovani, P.: 1995, *Publ. Astron. Soc. Pac.*, **107**, 803. https://doi.org/10.1086/133630

Volvach A., Volvach L., Larionov M.: 2023, *Galaxies*, **11**, 96. https://doi.org/10.3390/galaxies11050096

Yosuke, M.: 2022, *Universe*, **8**, 85. https://doi.org/10.3390/universe8020085

Zabora et al.: 2022, *AApTr*, **33**, 89. https://doi.org/10.17184/eac.6470